UCRL-JC-201671

LAWRENCE
LIVERMORE
NATIONAL
LABORATORY

Progress Towards High-Performance, Steady-State Spherical Torus

M. Ono et al.

January 2, 2004

For submission to Plasma Physics and Controlled Fusion

DISCLAIMER

This document was prepared as an account of work sponsored by an agency of the United States Government. Neither the United States Government nor the University of California nor any of their employees, makes any warranty, express or implied, or assumes any legal liability or responsibility for the accuracy, completeness, or usefulness of any information, apparatus, product, or process disclosed, or represents that its use would not infringe privately owned rights. Reference herein to any specific commercial product, process, or service by trade name, trademark, manufacturer, or otherwise, does not necessarily constitute or imply its endorsement, recommendation, or favoring by the United States Government or the University of California. The views and opinions of authors expressed herein do not necessarily state or reflect those of the United States Government or the University of California, and shall not be used for advertising or product endorsement purposes.

This is a preprint of a paper intended for publication in a journal or proceedings. Since changes may be made before publication, this preprint is made available with the understanding that it will not be cited or reproduced without the permission of the author.

This work was performed under the auspices of the U.S. Department of Energy by the University of California, Lawrence Livermore National Laboratory under Contract No, W-7405-Eng-48.

Progress towards high-performance, steady-state spherical torus

M Ono[1], M G Bell[1], R E Bell[1], T Bigelow[2], M Bitter[1], W Blanchard[1], J Boedo[3], C Bourdelle[4], C Bush[2], W Choe[5], J Chrzanowski[1], D S Darrow[1], S J Diem[6], R Doerner[3], P C Efthimion[1], J R Ferron[7], R J Fonck[6], E D Fredrickson[1], G D Garstka[6], D A Gates[1], T Gray[1], L R Grisham[1], W Heidbrink[8], K W Hill[1], D Hoffman[1], T R Jarboe[9], D W Johnson[1], R Kaita[1], S M Kaye[1], C Kessel[1], J H Kim[5], M W Kissick[6], S Kubota[10], H W Kugel[1], B P LeBlanc[1], K Lee[11], S G Lee[12], B T Lewicki[6], S Luckhardt[3], R Maingi[2], R Majeski[1], J Manickam[1], R Maqueda[13], T K Mau[3], E Mazzucato[1], S S Medley[1], J Menard[1], D Mueller[1], B A Nelson[9], C Neumeyer[1], N Nishino[14], C N Ostrander[6], D Pacella[15], F Paoletti[16], H K Park[1], W Park[1], S F Paul[1], Y-K M Peng[2], C K Phillips[1], R Pinsker[7], P H Probert[6], S Ramakrishnan[1], R Raman[9], M Redi[1], A L Roquemore[1], A Rosenberg[1], P M Ryan[2], S A Sabbagh[16], M Schaffer[7], R J Schooff[6], R Seraydarian[3], C H Skinner[1], A C Sontag[6], V Soukhanovskii[1], J Spaleta[1], T Stevenson[1], D Stutman[20], D W Swain[2], E Synakowski[1], Y Takase[17], X Tang[13], G Taylor[1], J Timberlake[1], K L Tritz[6], E A Unterberg[6], A Von Halle[1], J Wilgen[2], M Williams[1], J R Wilson[1], X Xu[18], S J Zweben[1], R Akers[19], R E Barry[2], P Beiersdorfer[18], J M Bialek[16], B Blagojevic[20], P T Bonoli[21], M D Carter[2], W Davis[1], B Deng[11], L Dudek[1], J Egedal[21], R Ellis[1], M Finkenthal[20], J Foley[1], E Fredd[1], A Glasser[13], T Gibney[1], M Gilmore[22], R J Goldston[1], R E Hatcher[1], R J Hawryluk[1], W Houlberg[2], R Harvey[23], S C Jardin[1], J C Hosea[1], H Ji[1], M Kalish[1], J Lowrance[24], L L Lao[7], F M Levinton[25], N C Luhmann[11], R Marsala[1], D Mastravito[1], M M Menon[2], O Mitarai[26], M Nagata[27], G Oliaro[1], R Parsells[1], T Peebles[10], B Peneflor[7], D Piglowski[1], G D Porter[17], A K Ram[19], M Rensink[17], G Rewoldt[1], J Robinson[1], P Roney[1], K Shaing[6], S Shiraiwa[20], P Sichta[1], D Stotler[1], B C Stratton[1], R Vero[16], W R Wampler[28] and G A Wurden[13]

[1] Princeton Plasma Physics Laboratory, Princeton University, New Jersey, USA
[2] Oak Ridge National Laboratory, Oak Ridge, Tennessee, USA
[3] University of California, San Diego, California, USA
[4] CEA Cadarache, France
[5] Korea Advanced Institute of Science and Technology, Taejon, Republic of Korea
[6] University of Wisconsin, Wisconsin, USA
[7] General Atomics, San Diego, California, USA
[8] University of California, Irvine, California, USA
[9] University of Washington, Seattle, Washington, USA
[10] University of California, Los Angeles, California, USA
[11] University of California, Davis, California, USA
[12] Korea Basic Science Institute, Taejon, Republic of Korea
[13] Los Alamos National Laboratory, Los Alamos, New Mexico, USA
[14] Hiroshima University, Hiroshima, Japan

[15] ENEA, Frascati, Italy
[16] Columbia University, New York, NY, USA
[17] Tokyo University, Tokyo, Japan
[18] Lawrence Livermore National Laboratory, Livermore, California, USA
[19] Euratom-UKAEA Fusion Association, Abingdon, Oxfordshire, UK
[20] Johns Hopkins University, Baltimore, Maryland, USA
[21] Massachusetts Institute of Technology, Cambridge, Massachusetts, USA
[22] University of New Mexico at Albuquerque, New Mexico, USA
[23] Compx, Del Mar, California, USA
[24] Princeton Scientific Instruments, Princeton, New Jersey, USA
[25] Nova Photonics, Princeton, New Jersey, USA
[26] Kyushu Tokai University, Kumamoto, Japan
[27] Himeji Institute of Technology, Okayama, Japan
[28] Sandia National Laboratories, Albuquerque, New Mexico, USA

Abstract

Research on the spherical torus (or spherical tokamak) (ST) is being pursued to explore the scientific benefits of modifying the field line structure from that in more moderate aspect ratio devices, such as the conventional tokamak. The ST experiments are being conducted in various US research facilities including the MA-class National Spherical Torus Experiment (NSTX) at Princeton, and three medium sized ST research facilities: PEGASUS at University of Wisconsin, HIT-II at University of Washington, and CDX-U at Princeton. In the context of the fusion energy development path being formulated in the US, an ST-based Component Test Facility (CTF) and, ultimately a Demo device, are being discussed. For these, it is essential to develop high performance, steady-state operational scenarios. The relevant scientific issues are energy confinement, MHD stability at high beta (β), non-inductive sustainment, Ohmic-solenoid-free start-up, and power and particle handling. In the confinement area, the NSTX experiments have shown that the confinement can be up to 50% better than the ITER-98-pby2 H-mode scaling, consistent with the requirements for an ST-based CTF and Demo. In NSTX, CTF-relevant average toroidal beta values β_T of up to 35% with a near unity central β_T have been obtained. NSTX will be exploring advanced regimes where β_T up to 40% can be sustained through active stabilization of resistive wall modes. To date, the most successful technique for non-inductive sustainment in NSTX is the high beta poloidal regime, where discharges with a high non-inductive fraction ($\sim$60% bootstrap current+NBI current drive) were sustained over the resistive skin time. Research on radio-frequency (RF) based heating and current drive utilizing high harmonic fast wave and electron Bernstein wave is also pursued on NSTX, PEGASUS, and CDX-U. For non-inductive start-up, the coaxial helicity injection, developed in HIT/HIT-II, has been adopted on NSTX to test the method up to $I_p \sim 500$ kA. In parallel, start-up using a RF current drive and only external poloidal field coils are being developed on NSTX. The area of power and particle handling is expected to be challenging because of the higher power density expected in the ST relative to that in conventional aspect-ratio tokamaks. Due to its promise for power and particle handling, liquid lithium is being studied in CDX-U as a potential plasma-facing surface for a fusion reactor.

1. Introduction

The spherical torus (ST) [1] research conducted worldwide has made remarkable progress in recent years. In the US, ST experimental research is being carried out in several facilities including National Spherical Torus Experiment (NSTX) [2] and CDX-U [3] at Princeton Plasma Physics Laboratory (PPPL), PEGASUS [4] at University of Wisconsin, and HIT-II [5] at University of Washington. Within the US ST research effort, the Innovative Confinement Concept (ICC) programme, the Innovative Diagnostic Development programme, the US theory programme and the Virtual Laboratory for Technology programme are four crucial elements. The ST programme, at present, focuses on two broad goals. The first goal is to assess the attractiveness of the ST as a fusion energy concept such as the ST-based Component Test Facility (CTF) and Demo. The US ST programme is indeed well aligned with the recently developed fusion energy development path plan [6]. The second goal is to use ST plasma characteristics to foster a deeper understanding of critical toroidal physical issues.

2. Scientifically important ST issues

The ST configuration offers the following physical conditions to develop a deeper understanding of high temperature toroidal plasmas as well as astrophysical plasmas:

- High average toroidal beta $\langle\beta_{\mathrm{T}}\rangle$ of ~40% and order unity central beta β_0. Because of the favourable MHD stability at low aspect ratios, $A = R/a < 2$ [1], the ST plasmas have already accessed a high average toroidal beta of 35–40% and a central beta of the order of unity. This property permits fusion power production at a relatively low confining toroidal field and, thus, reduces the cost of the power plant and recirculating power. The unity beta condition is also relevant for the physics of space plasmas.
- Strong plasma shaping and self-fields ($A \geqslant 1.27, \delta \leqslant 0.8, \kappa \leqslant 2.5, B_{\mathrm{P}}/B_{\mathrm{T}} \sim 1$). Because of the strong toroidicity and shaping produced in ST plasmas, research in these extreme conditions could lead to an improved and deeper understanding of all toroidal plasmas.
- Large plasma Mach number ($V_{\mathrm{rotation}}/V_{\mathrm{A}} \sim 0.3$). Since for beta equal to unity, the Alfvén velocity V_{A} approaches the ion thermal velocity, it is relatively easy to access high Alfvén Mach number plasmas. This property could relax the condition for wall stabilization by plasma rotation for the ST reactor.
- Large flow shearing rate ($\gamma_{E\times B} \leqslant 10^6\ \mathrm{s}^{-1}$). With strong plasma rotation and toroidicity, ST plasmas could generate significant sheared flows, which could suppress the long wavelength turbulence to improve confinement.
- Supra-Alfvénic fast ions ($V_{\mathrm{fast}}/V_{\mathrm{A}} \sim 4$–5). Again, this condition can be readily created because of the low Alfvén velocity of ST. The wave–particle interactions in this regime could be of relevance to the alpha particle physics in burning plasmas such as ITER.
- High dielectric constant ($\varepsilon \sim 50$). The high plasma dielectric constant drastically modifies the propagation characteristics of some plasma waves. While this property excludes using certain types of plasma waves such as ECH and lower hybrid waves, it gives rise to new opportunities for waves such as high harmonic fast waves (HHFWs) and electron Bernstein waves (EBWs).
- Large mirror ratios in the edge B field. Near the plasma boundary, the toroidal field could vary by as much as a factor of 5, producing a large mirror ratio. This property can modify the edge power flow.

3. Physical requirements for steady-state high-performance plasmas

It is important to note that the unique physical properties of the ST described above could also help the ST achieve its long-range goal of steady-state operation at high performance which is needed for ST-based reactors. The physical requirements for ST fusion systems can be summarized as follows:

- MHD stability at high β_T and β_N: to produce the required fusion power at low toroidal fields, a high β is needed. Since the self-driven current fraction is proportional to $\varepsilon\beta_P \equiv \varepsilon 2\mu_0\langle p\rangle/B_P^2$ and $\beta_T \propto \beta_N^2/\beta_P$, a very high value of normalized beta, β_N, is needed for a high bootstrap current fraction. Typically, $\beta_T \sim 20\%$, $\beta_N \sim 6$ is needed for CTF and much more challenging $\beta_T \geqslant 40\%$, $\beta_N \sim 8$ is needed for Power Plants (e.g. ARIES-ST). This power plant regime will require advanced ST operations with plasma beta near the ideal stability limits and, therefore, is likely to require some kind of active feedback stabilization of MHD modes.
- Transport and confinement: since the fusion power production is a very strong function of the plasma confinement (P_{fusion} is proportional to the H-factor to as much as the seventh power), it is important to understand the confinement trends and improve the predictive capability of confinement. The systems code studies of ST-based CTF and Power Plant design suggest that the required global confinement should be in the range, $H_{98\text{pby},2} \sim 1.4$–$1.7$.
- Power and particle handling: because of the small major radius of ST reactors, the expected P/R is much larger than that of conventional fusion reactors by a factor of ~2–3. While, this is a stringent requirement, the unique ST geometry may provide a solution to this problem in terms of large flux expansion together with an innovative solution for the plasma facing component (PFC), such as liquid lithium.
- Solenoid-free start-up: the elimination of the in-board solenoid is required for the ST to be an attractive fusion power plant, since an in-board solenoid, along with the shielding needed for its insulation, increases the size and, hence, the cost of the plant. Thus, ST-based fusion systems including the CTF and power plant designs, assume complete elimination of the central solenoid.
- Integrating scenarios: while it is often logical and convenient to explore each physical requirement independently to facilitate understanding, it is necessary to demonstrate all the essential aspects of the physical requirements simultaneously in an integrated manner for a credible fusion system.

4. US ST facilities

There are four US ST facilities. The NSTX at the PPPL is a 1 MA class facility designed to evaluate the physical principles of the ST. The NSTX facility efficiently utilized the TFTR site capability in terms of power supplies and auxiliary heating systems to optimize the facility. There are three smaller facilities dedicated to study targeted innovative ST research areas. The PEGASUS facility at University of Wisconsin is a few 100 kA class facility designed to investigate the very low aspect ratio region and aimed to bridge the physical gap between spheromaks and STs. The HIT-II facility is also a few 100 kA class facility dedicated to develop an innovative non-inductive plasma start-up concept based on coaxial helicity injection (CHI). The CDX-U facility at PPPL is now focusing its efforts to test lithium coating and liquid lithium PFCs to develop attractive power and particle handling methods for STs. Table 1 shows the parameters achieved in the four facilities.

Table 1. Achieved key device parameters for the US ST facilities.

Devices	NSTX	PEGASUS	HIT-II	CDX-U
I_p (MA)	1.5	0.2	0.26	0.1
R (m)	0.86	0.25–0.45	0.3	0.33
$A(\equiv R/a)$	1.26	1.2	1.5	1.5
$B_T R$ (T m)	0.5	0.03	0.15	0.07
τ-pulse (s)	1.1	0.1	0.1	0.025
Elongation	2.2	1–3.5	1.5	1.55
OH flux (Wb)	0.7	0.1	0.06	0.1
NBI (MW)	7			
HHFW (MW)	6	1		0.1
CHI (MA)	0.4		0.2	

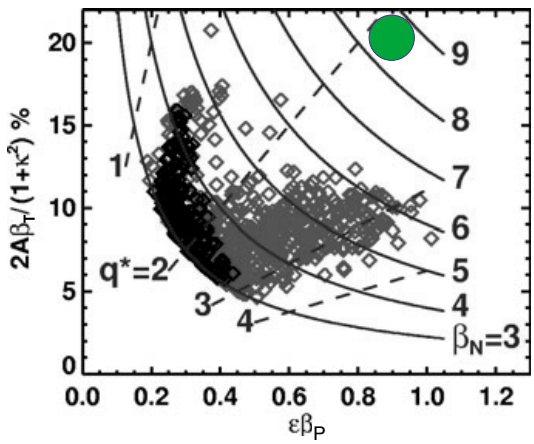

Figure 1. Normalized plasma toroidal beta vs normalized plasma poloidal beta. The black diamond is data from the 2001 run and the red (light colour) diamonds are from the 2002 run. The normalized beta contours are as labelled. The target beta regime is shown as a large circle.

5. Progress on MHD stability at high β_T and β_N in NSTX

The beta limit investigations were conducted mainly in NSTX due to its strong auxiliary heating capability [7]. The PEGASUS device also investigated the plasma beta with Ohmic heating taking advantage of the low-aspect ratio geometry as described below. In figure 1, the normalized β_T achieved vs normalized β_{pol} data points are shown. In 2001, rapid progress was made to reach $\beta_T \sim 25\%$, which is near the so-called no-wall beta limit, i.e. in the absence of the stabilizing effects of a nearby conducting wall as shown by the black diamonds. In 2002, after re-aligning the outer poloidal field coils, the $n = 1$ error field component was reduced by a factor of 10. This error field reduction improved the plasma beta values dramatically as shown in the figure by the red (or lighter) diamonds. The maximum β_T value increased to 35% and the maximum β_{pol} value doubled from 0.6 to 1.4. The data point for a β_T of 35% ($\kappa = 2$, $A = 1.38$) is shown by the highest data point in the vertical scale in the figure. This improvement was also aided by the ready access to the H-mode, which broadened the pressure profiles, which in turn improves MHD stability [8]. Analysis of many plasmas with high β_N indicates that the no-wall stability limit has indeed been exceeded, and that wall stabilization is a critical player in achieving these high beta states [9]. In figure 2, the evolution of the $\beta_T \sim 35\%$ shot is shown. As can be seen from the figure, the discharge reached $\beta_T = 35\%$ shortly after entering H-mode. The presence of an $n = 1/m = 1$ mode seems to regulate the beta value and maintained the high beta value for a period larger than the energy confinement time until the

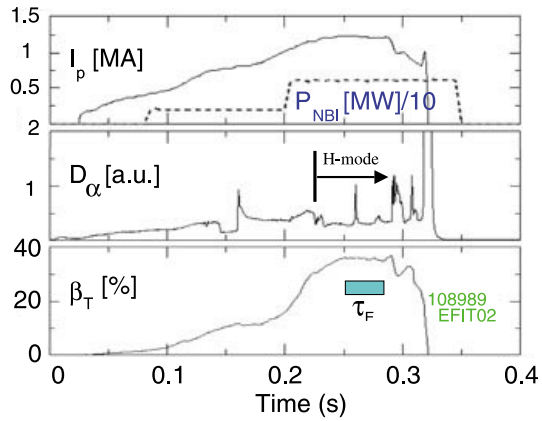

Figure 2. The discharge evolution of the $\beta_T = 35\%$ discharge is shown.

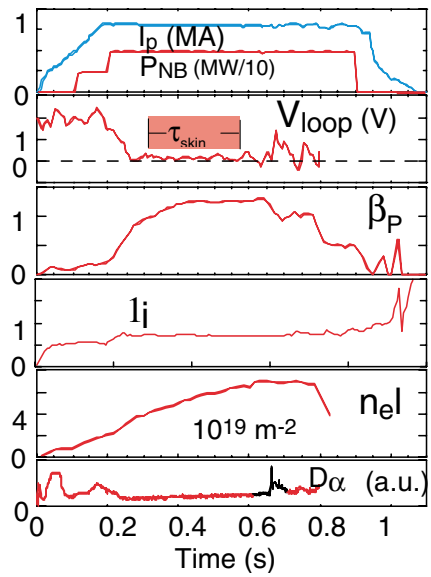

Figure 3. The discharge evolution of the high β_P shot.

end of the current flat-top. In figure 3, we show the high poloidal beta shot at 800 kA. As can be seen, the loop voltage drops from 2 V to about 0.1 V around $t = 0.3$ s coincident with the rise in β_P. The non-inductive current drive fraction is calculated to be about 60% due to the bootstrap currents and NBI current drive in this phase. The plasma internal inductance l_i stays nearly constant for about 400 ms, much longer than the plasma current skin time of ~200 ms. The H-mode which kept the pressure profile broad and q-minimum (calculated by EFIT) to stay around 2, contributed to the MHD stability. The rapid plasma rotation contributed to the stability through wall stabilization allowing the plasma to stay above the no-wall stability limit for many tens of wall resistive times of ~10 ms. The achieved parameters $\beta_N \times H_{89P} \sim 15$ with $\beta_T \sim 15\%$ of the high poloidal beta discharges is already comparable to that which is required for CTF. The plasma density, however, rises continuously, which indicates that the particle control is an issue that must be addressed in order to realize a truly steady-state regime [10].

6. PEGASUS high beta experiment

High toroidal beta plasmas are obtained in PEGASUS by operation at very low toroidal fields, and cover a region of the β_T vs I_N space similar to neutral-beam heated high-β_T plasmas

in START and other ST experiments (figure 4) [4]. As indicated, β_T values up to 25% and $\beta_N \sim 5$ have been obtained with no evidence of a beta limit to date. Densities range up to the Greenwald limit ($\sim I_p/\pi a^2$). Stored energies are consistent with values expected from the ITER-98pby confinement scaling. Plasma start-up is characterized by high current ramp rates (15–45 MA s^{-1}), low internal inductance ($l_i \sim 0.3$), and high elongation. Two-dimensional images of x-ray emission from PEGASUS plasmas have enabled, for the first time, a non-perturbative measurement of the plasma current profile in a ST [4]. This measurement is accomplished by determining intensity contours from the image and using the contours as inputs in the solution of the MHD equilibrium state. The shape of the contours is a strong constraint on the current profile and thus the q-profile in the equilibrium reconstruction. The resulting q-profile shows near-zero central shear. Plasmas with $\beta_T \sim 1$ as A approaches unity in the tokamak–spheromak overlap region appear accessible with the addition of planned new capabilities, which are aimed at lowering the plasma resistivity and manipulating the evolution of the q-profile to suppress limiting MHD activity. These include high-power radio-frequency (RF) heating, a transient increase in the toroidal field for a stabilized formation stage, loop voltage control and significantly increased Ohmic volt-seconds, an upgraded equilibrium field system for shape and position control, and separatrix operation. Operation with a two-strap high-power higher harmonic fast wave heating system has begun. Initial loading tests show an impedance of 1 Ω, and up to 200 kW has been injected to date. Tokamak simulation code (TSC) modelling of fast TF rampdown scenarios indicate accessible paths to regimes of higher current and increased stored energy.

7. Supra-Alfvénic fast ion induced high frequency MHD

Owing to high beta, the ST plasmas provide a good test bed to investigate wave–particle interactions for the supra-Alfvénic fast ions ($V_{NBI}/V_A \sim$ 4–5). This type of regime is similar to those encountered for alpha-heated discharges such as ITER. In the NSTX NBI heated discharges, a wide variety of high frequency MHD instabilities has been detected at frequencies ranging from a few kHz to many MHz [11–13]. In the frequency range below about 200 kHz, a form of fishbone or energetic particle modes has been seen, as well as modes that appear to be similar to the toroidal Alfvén eigenmode (TAE) of conventional tokamaks. Unlike in conventional tokamaks, the frequency ranges of these two classes of instabilities have substantial overlap, complicating the experimental identification and theoretical analysis. Significant fast ion losses have been correlated, under some conditions, with the appearance of both these types of modes.

8. Progress on transport and confinement

The global confinement times in neutral beam heated NSTX plasmas compare favourably with the ITER-89P empirical scaling expression as well as the ITER-98(pby, 2) scaling rule [14, 15]. In recent years, H-mode operation has become routine on NSTX, aided by improved wall conditioning and reduced error fields. Access to the H-mode is easiest in the lower single null (LSN) configuration, but H-modes have been obtained in double null as well. The power threshold is several hundred kW and exhibits a secular fall as wall conditions improve. Gas injection on the high field side produces H-mode access more easily compared to low field side gas injection [8]. In figure 5, NSTX H-mode experimental confinement data points obtained in quasi-steady conditions are shown compared to the ITER-98py2 H-mode scaling. The solid circles are the global confinement times and the diamonds are the confinement with energetic component and NBI prompt loss components removed. The

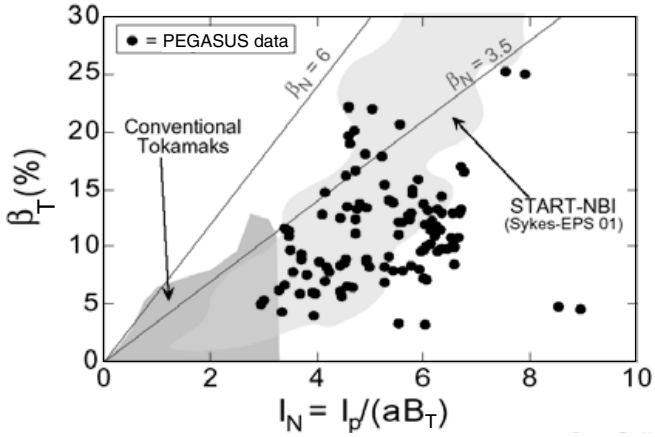

Figure 4. Toroidal beta vs normalized current for Ohmically heated PEGASUS discharges.

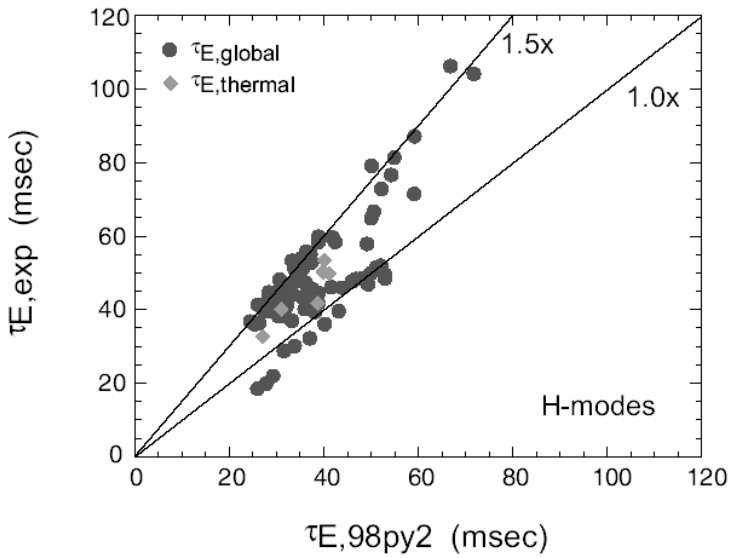

Figure 5. NSTX H-mode experimental confinement data points are shown compared to the ITER-98pby2 H-mode scaling. The circular (red) points are the global confinement times and the diamonds (green) are the confinement with energetic component and NBI lost components removed.

H-mode data shows up to 50% global confinement improvement compared to the H-mode scaling. The level of confinement enhancement is comparable to that which is needed for future ST devices. The global confinement scaling study has begun on NSTX. The accurate determination of R/a dependence is an active International Tokamak Physics Activity (ITPA) research topic. The L-mode data show a similar scaling to that in the conventional aspect ratio tokamaks $\tau_E^{\text{NSTX-L}} \sim I_{\text{p}}^{0.76} B_{\text{T}}^{0.27} P_{\text{L}}^{-0.76}$. The H-mode data, on the other hand, show less power degradation $P^{-0.5}$, which is encouraging. But it should also be noted that the H-mode parametric dependences are turning out to be more complex and non-linear, showing the need for further refinement of this low-aspect-ratio high beta ST regimes.

9. Transport diffusivities

The power balance analysis of the NSTX NBI heated discharges is shown in figure 6. The ion thermal conductivity χ_{i} appears to track the predictions from neoclassical theory quite well, and the electron thermal conductivity χ_{e} is significantly larger than χ_{i}. The momentum diffusivity

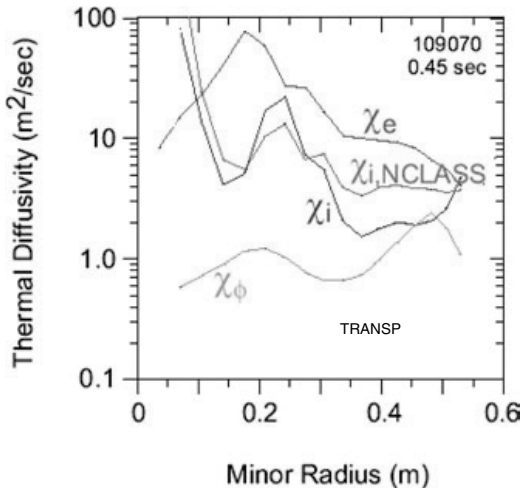

Figure 6. Thermal and momentum diffusivities as labelled calculated from TRANSP power balance calculations. Shown for comparison is the calculated neoclassical thermal diffusivity from the NCLASS neoclassical model. The plasma radius is about 65 cm.

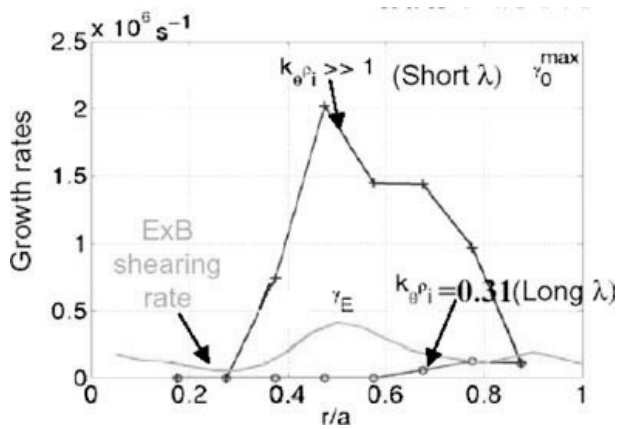

Figure 7. Growth rates computed by GS2 show that the $E \times B$ shearing rate exceeds long wavelength modes thereby stabilizing them. The short wavelength modes on the other hand may dominate (electron) transport.

χ_ϕ is much smaller than χ_i in this analysis, qualitatively consistent with expectations from neoclassical theory. The observed ordering is therefore $\chi_\phi < \chi_i \leqslant \chi_{neo} < \chi_e$. In general, the observed diffusivity profiles are unusual in that the thermal diffusivities decrease with the minor radius. This type of diffusivity profile tends to give broader pressure profiles, which is favourable for plasma high beta stability. Owing to the small χ_ϕ, the NSTX plasma rotates relatively rapidly at 200–300 km s^{-1} reaching a rather high Mach number of $V_{rotation}/V_A \sim 0.3$. The improved ion confinement appears to be indeed correlated with the plasma rotation. The plasma rotation could also provide a stabilizing influence on the MHD modes, as discussed earlier. The observed $\chi_i \sim \chi_{neo}$ and $\chi_\phi < \chi_i$ suggest that long wavelength turbulence may be suppressed. In order to develop a fundamental understanding of the plasma transport, a variety of theoretical tools are utilized. The growth rates computed by a gyro-kinetic based transport modelling code (GS2) indeed show that the $E \times B$ shearing rate is sufficiently higher than the predicted growth rates of ion temperature gradient (ITG) mode range turbulence as shown in figure 7, consistent with the low ion thermal diffusivity [16, 17]. In the electron temperature gradient (ETG) mode range of short wavelength modes, the linear instability growth rate is significantly larger than the shearing rate, consistent with the relatively large observed χ_e.

This neoclassical ion transport regime can provide a unique test bed to investigate the electron transport physics in NSTX.

10. Progress on power and particle handling

The NSTX boundary physical research thus far focused on power and particle balance [10]. High heat flux on the target plate has been measured in LSN divertor plasmas. The peak heat flux in a LSN ELM-free H-mode plasma with 4.5 MW of heating power has reached 10 MW m^{-2}, with a full-width at half-maximum of 2 cm at the outer target plate, approaching the spatial resolution of the IR camera used to make the measurement. The peak heat flux in H-mode plasmas increases with NBI heating power. The peak heat flux at the inboard target is typically 0.5–1.5 MW m^{-2}, with a profile full-width at half-maximum of ~10 cm. The power flowing to the inboard side is typically 0.2–0.33 of the outboard power. Similar in–out asymmetry ratios have been observed in the MAST device [18]. Double-null high triangularity discharges appear to have a much lower peak heat flux than LSN discharges. A preliminary measurement is shown in figure 8, which shows a much lower heat flux, ~3 MW m^{-2}, consistent with the greater flux expansion for the high triangularity discharges, as shown in figure 8. This is a promising result, which can be used to minimize the peak heat load on the divertor plates. It should be noted that the ARIES-ST configuration also assumes a similar high triangularity configuration to reduce the divertor peak heat load to an acceptable level.

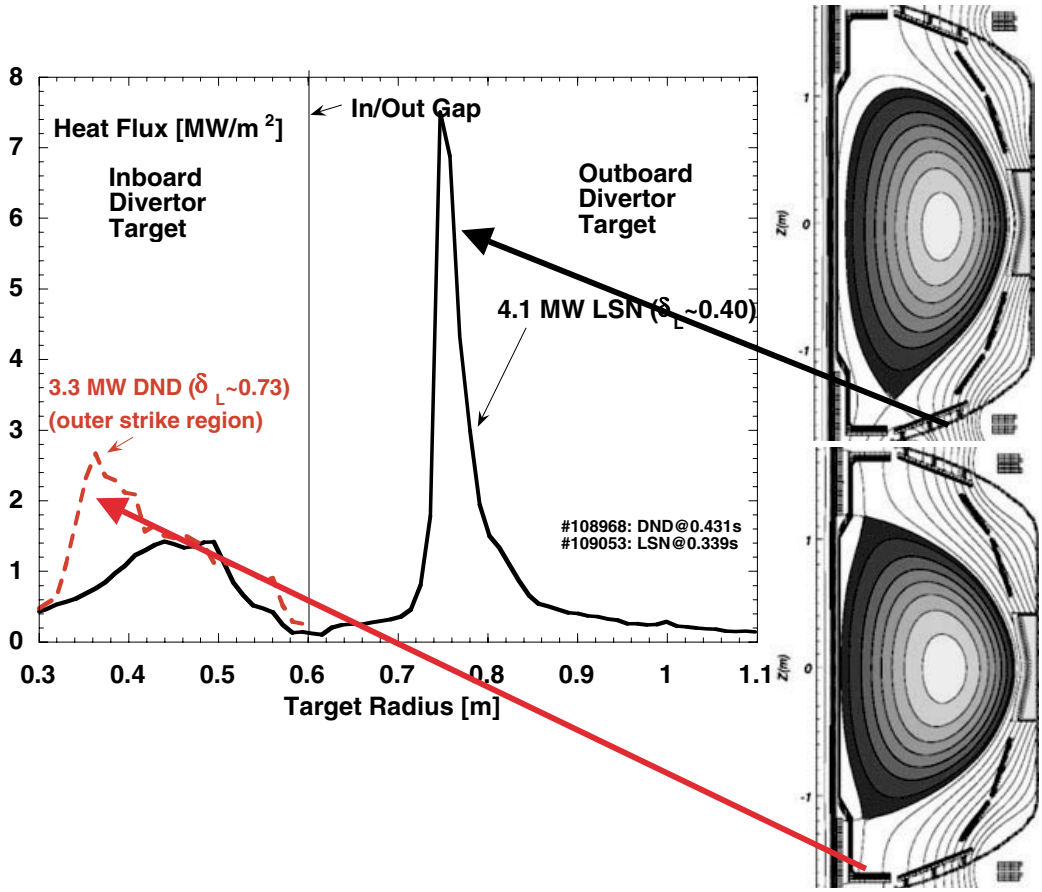

Figure 8. Divertor heat load flux comparison for the single null and the high triangularity double null discharges.

11. Liquid lithium limiter experiment on CDX-U

The primary research topic under investigation on CDX-U is the use of liquid metals, and in particular liquid lithium, as PFCs for the ST and tokamak. The primary motivation for these experiments is a test of liquid metal PFCs as a potential engineering solution to the problems of high heat flux and erosion of the first wall, which is expected in a reactor. However, liquid lithium PFCs have attractive physical advantages as well. A shallow toroidal tray, which encircles the centrestack and forms the lower limiting surface for the plasma, has been installed in the vessel. The tray has a major radius of 34 cm, is 10 cm wide and 0.5 cm deep, and is fitted with heaters to allow operation at temperatures up to 500°C; the typical temperature during tokamak operation is 300°C. The tray has been filled with ≈1 litre of liquid lithium; a photograph of part of the tray, installed in CDX-U and filled with (highly reflective) liquid lithium is shown in figure 9. Plasma operation with a bare stainless steel tray and with a liquid lithium-filled tray has been compared. The use of liquid lithium as a limiter material results in a significant reduction in the oxygen impurity in the discharge. Recycling is reduced during lithium operation, resulting in the requirement of an eightfold increase in the gas puffing rate in order to maintain a plasma density comparable to discharges with the bare, fully recycling, stainless steel tray. The plasma loop voltage during lithium operation is reduced from 2 to 0.5 V at a comparable plasma current. This is consistent with the change in Z_{eff} from about 3 to ≈1. The lithium remains quiescent and is confined to the tray during plasma operation. The performance enhancement produced by the use of lithium as a PFC is far more evident than improvements produced by titanium gettering or boronization in CDX-U. Because of the encouraging results from CDX-U, NSTX will be testing the lithium techniques to solve the heat and particle issues.

12. Progress on solenoid-free start-up

Due to the importance of solenoid-free start-up research for the ST, NSTX is investigating two alternative approaches for the central-solenoid-free start-up. The first one is the CHI developed by the HIT-II group at University of Washington [5]. The other is the outer PF coil start-up concept.

12.1. Coaxial helicity injection

This CHI concept is an outcome of the spheromak research. A number of smaller helicity injection experiments were performed with some success prior to introducing it on NSTX. On NSTX, CHI has already produced about 400 kA of toroidal current with a record current amplification of 14 accompanied by distinct $n = 1$ relaxation activities [19]. The CHI short term research goal is to establish an understanding of the current penetration process and to confirm the existence of closed flux surfaces and to demonstrate coupling of the CHI produced current to other non-inductive current drive methods. Theoretical modelling of CHI has been pursued with a three-dimensional MHD code to understand the reconnection processes during CHI [20].

12.2. Transient CHI in HIT-II

To complement the so-called slow CHI start-up research, an innovative transient CHI start-up method has been developed recently on the HIT-II device [5]. By applying a short pulse CHI bias voltage, one can create a high quality (low impurity) CHI discharge, which can detach from the electrode and form a closed flux surface discharge. This well formed, clean CHI

Figure 9. View of the lithium-filled toroidal tray in CDX-U through a port. The centrestack is the vertical column in the left side of the field of view. The tray is indicated by the arrow. Note the highly reflective surface, indicative of the liquid lithium in the tray.

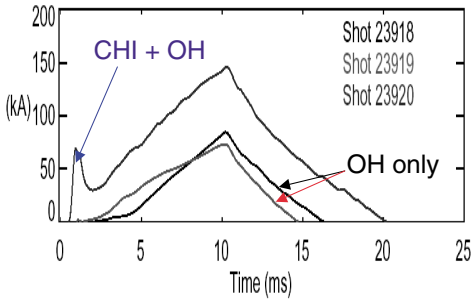

Figure 10. Comparison of CHI + OH and OH only discharges as labelled. For all discharges a constant inductive voltage of 4 V is applied for 2 ms, followed by 3.2 V for the next 6.8 ms.

discharge provides an ideal target for induction. As shown in figure 10, this method indeed saves poloidal flux and produces a much higher current than the induction only case. Using this method, the HIT-II produced a record plasma current of 265 kA. This method will be tested on NSTX. If it works well, one can apply RF heating and current drive to make the plasma start-up and ramp-up completely non-inductive.

12.3. Outer-poloidal-field-coil start-up

While it is very difficult to build a central solenoid for the ST due to limitations of space, the ST geometry offers an interesting possibility to utilize the outer PF coils for solenoid-free start-up [21]. By appropriately controlling the outer PF coil currents, one can create a high quality field null as shown in figure 11. Using a maximum coil current of 20 kA, this method can generate up to 10 V of loop voltage while retaining a good quality field null for the required duration of 3 ms. The Lloyd condition with strong pre-ionization ($E_T B_T / B_P > 0.12\,\mathrm{kV\,m^{-1}}$) can be satisfied for a large plasma volume [22]. The available flux for this case is about 120 mWb, which may be sufficient for generating about 300 kA of plasma current in NSTX. If the Lloyd condition can be relaxed further using strong heating and current drive as observed on JT-60U [23], the flux availability for this method can be further increased. This poloidal field coil start-up will be tested on NSTX since, if proven, it can be readily applied in future devices.

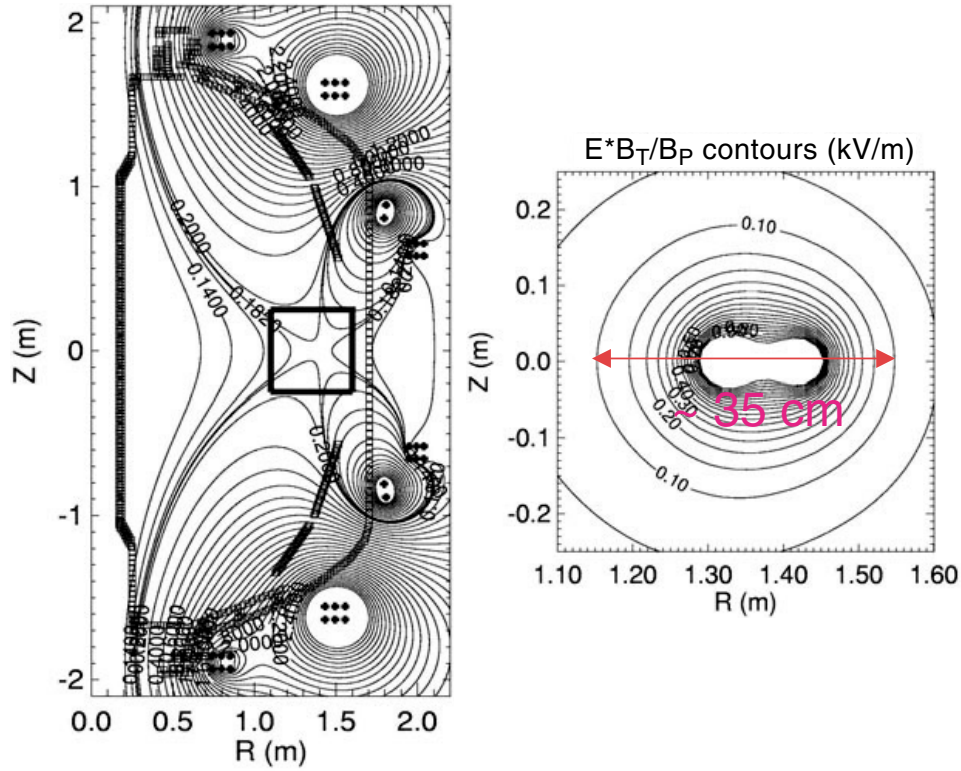

Figure 11. The NSTX outer PF-only high quality null formation. (*a*) Flux contours. (*b*) $E_T B_T / B_P$ contours in kV m^{-1} at the time of initiation.

13. Progress on integrating scenarios

As mentioned earlier, while it is often logical to explore each physical requirement independently to facilitate understanding, it is necessary to demonstrate all the essential aspects of the physical requirements simultaneously in an integrated manner for a credible fusion system. In order to achieve the ST reactor relevant physical goals of 40% β_T, $I_{NI} = 100\%$, and $\tau_{pulse} \gg \tau_{skin}$, the following additional modifications are planned on NSTX.

- Enhanced shaping improves MHD stability. As shown in figure 12, the achieved beta values tend favourably towards higher triangularity and higher elongation regimes. One of the modifications of inner PF coils planned in NSTX will permit the investigation of the $\kappa = 2.4$ and $\delta = 0.8$ regime. This favourable trend is consistent with the MHD stability calculations predicting stable 40% β_T, and full non-inductive current sustainment, $I_{NI} = 100\%$, for the $\kappa = 2.4$ and $\delta = 0.8$ regime.
- Since the 40% β_T and $I_{NI} = 100\%$ regime requires wall stabilization, NSTX will install active feed back coils to explore the regime approaching the ideal wall limit using the active coil system together with plasma rotation.
- In order to achieve $\tau_{pulse} \gg \tau_{skin}$ in the advanced regime, it is important to control heat and particles. The maintenance of a moderate plasma density is important for an efficient current drive. NSTX plans to install divertor lithium wall coating and a cryo-pump system to control the particle exhaust. Improved fuelling using supersonic gas injection and advance fuelling techniques are also planned.
- The existing 6 MW of HHFW heating [24] will contribute both to bootstrap current by raising T_e and to direct current drive. The electron heating by HHFW has been demonstrated as shown in figure 13(*a*) where an electron internal transport barrier was formed and resulted in a high T_e regime. In figure 13(*b*), the current drive was demonstrated

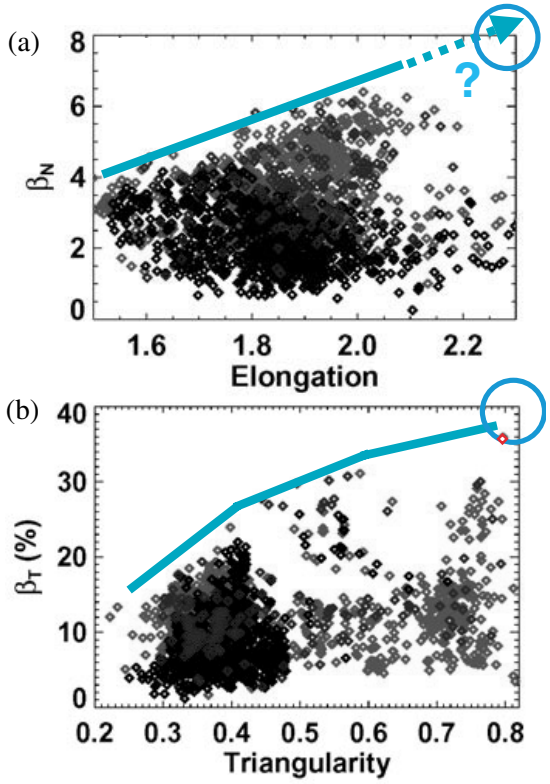

Figure 12. Achieved plasma beta values vs plasma shaping parameters. The black, red, and blue diamonds are data from the 2001, 2002, and 2003 campaign, respectively. (*a*) β_N vs plasma elongation. (*b*) β_T vs plasma triangularity.

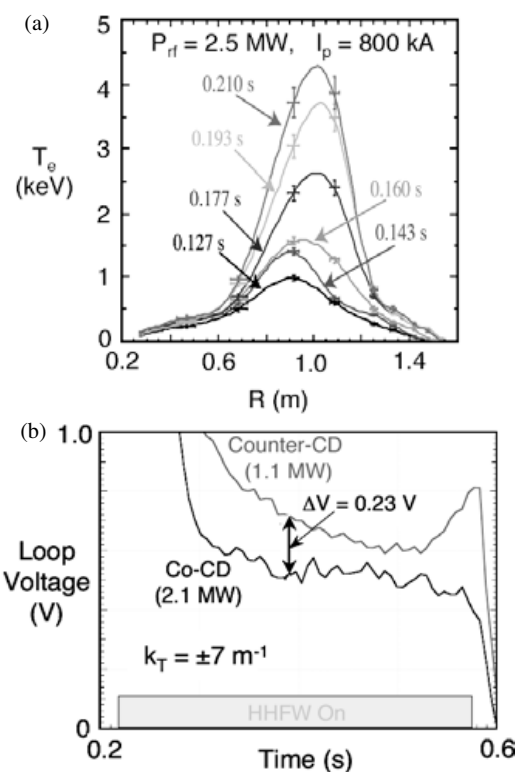

Figure 13. HHFW heating and current drive in NSTX. (*a*) Strong central heating by HHFW with creation of electron transport barrier. (*b*) Differences in V_{loop} with co- and counter-directed waves indicate ~100 kA of current drive consistent with theoretical modelling estimate.

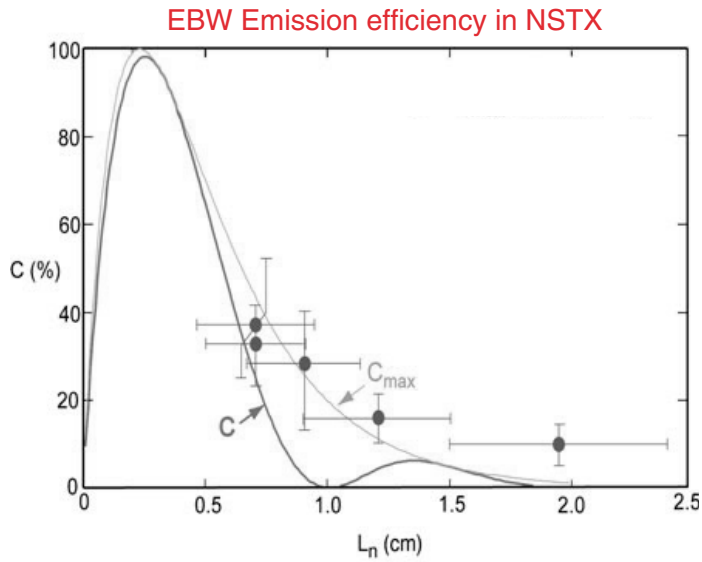

Figure 14. Observed EBW emission coefficient in NSTX. The curves are theoretical values.

by confirming differences in V_{loop} with co- and counter-directed waves maintained for over the current skin-time [25]. The observed V_{loop} differences can be attributable to ~100 kA of driven current which is consistent with a theoretical estimate. However, a theoretical modelling calculation indicates that HHFW off-axis CD efficiency may be reduced in the high thermal-ion beta regimes due to the energetic and bulk ion absorption and trapping effects. The energetic ion interaction with HHFW has been observed on NSTX [26].

- The advanced regime also requires an off-axis current drive of ~100 kA (out of $I_{\text{p}} \sim 1$ MA) to maintain the central $q \sim 2$. A 4 MW 15 GHz EBW system is planned to provide the necessary off-axis CD as well as localized CD to stabilize neoclassical tearing modes as needed. EBW appears not to suffer from parasitic ion absorptions as in the case of HHFW. It should also be noted that recent calculations indicate that the so-called Ohkawa current (which is induced by trapping the barely passing particles through perpendicular heating) can greatly enhance the EBW driven current efficiency in the off-axis regions due to the large trapped particle populations in the ST plasmas. The calculated efficiency $\zeta_{\text{ec}} = 0.4$ at large $r/a > 0.5$ compares favourably to ECCD and HHFWCD. The EBW launching efficiency can be optimized using the EBW emission measurements since the process is reversible. As shown in figure 14, the EBW emission measurements in NSTX agrees well with the theoretical calculations [27]. It is believed that by controlling the edge density gradient, the coupling efficiency can be raised 100% as demonstrated in CDX-U [28].

14. Conclusions and discussion

ST research is making rapid progress. In the MHD area, NSTX achieved 35% β_{T} with NBI heating and PEGASUS achieved 25% β_{T} with just Ohmic heating. NSTX also reached the high β_{P} regime (I_{NI} fraction ~60%) with $\beta_{\text{N}} H_{89\text{p}} = 15$ at $\beta_{\text{T}} = 15\%$ sustained over τ_{skin}. The β and confinement parameters achieved are comparable to that which is needed for CTF. Neoclassical-like ion confinement was observed in NBI heated discharges with $H_{98\text{pby},2} \sim 1.4$. Very low χ_ϕ led to a rapid plasma rotation with $V_{\text{rotation}} \sim 0.3 V_{\text{A}}$. The shear flow stabilization of long wavelength ITG modes is consistent with the observation. The high-triangularity double-null configuration shows a large reduction in peak heat flux. The CDX-U liquid lithium limiter

experiment yielded encouraging results. Two innovative plasma start-up concepts using the CHI method developed by HIT-II and outer poloidal field coils are presented. A number of new tools are planned to access the ST power plant relevant advanced regimes of 40% β_T and 100% non-inductive current drive through strong plasma shaping ($\delta \sim 0.8$, $\kappa \sim 2.4$) and profile control.

Acknowledgments

This research was supported by DoE contract DE-AC02-76CH03073 and DoE Grant DE-FG02-96ER54375.

References

[1] Peng Y-K M and Strickler D J 1986 *Nucl. Fusion* **26** 576
[2] Synakowski E J *et al* 2003 **43** at press
[3] Majeski R *et al* 2003 *J. Nucl. Mater.* **313–316** 625
[4] Garstka G D *et al* 2003 *Phys. Plasmas* **10** 1705
[5] Raman R *et al* 2003 *Phys Rev. Lett.* **90** 075005-1
[6] FESAC Panel of Development Path 2003 A Plan for the Development of Fusion Energy *Final Report to FESAC*
[7] Menard J *et al* 2003 *Proc. 30th Conf. on Plasma Physics and Controlled Fusion (St Petersburg, Russia, 7–11 July) (Europhysics Conference Abstracts)*
[8] Maingi R *et al* 2003 *Proc. 30th Conf. on Plasma Physics and Controlled Fusion (St Petersburg, Russia, 7–11 July) (Europhysics Conference Abstracts)*
[9] Sabbagh S *et al Proc. 19th IAEA Meeting (Lyon, France, 2002) Nucl. Fusion* submitted
[10] Soukhanovskii V A *et al* 2003 *Proc. 30th Conf. on Plasma Physics and Controlled Fusion (St Petersburg, Russia, 7–11 July) (Europhysics Conference Abstracts)*
[11] Fredrickson E *et al* 2003 *Proc. 30th Conf. on Plasma Physics and Controlled Fusion (St Petersburg, Russia, 7–11 July) (Europhysics Conference Abstracts)*
[12] Gorelenkov N *et al* 2003 *Proc. 30th Conf. on Plasma Physics and Controlled Fusion (St Petersburg, Russia, 7–11 July) (Europhysics Conference Abstracts)*
[13] Belova E *et al* 2003 *Proc. 30th Conf. on Plasma Physics and Controlled Fusion (St Petersburg, Russia, 7–11 July) (Europhysics Conference Abstracts)*
[14] LeBlanc B *et al* 2003 *Proc. 30th Conf. on Plasma Physics and Controlled Fusion (St Petersburg, Russia, 7–11 July) (Europhysics Conference Abstracts)*
[15] Stutman D *et al* 2003 *Proc. 30th Conf. on Plasma Physics and Controlled Fusion (St Petersburg, Russia, 7–11 July) (Europhysics Conference Abstracts)*
[16] Bourdelle C *et al* 2003 *Phys. Plasmas* submitted
[17] Redi M *et al* 2003 *Proc. 30th Conf. on Plasma Physics and Controlled Fusion (St Petersburg, Russia, 7–11 July) (Europhysics Conference Abstracts)*
[18] Akers R *et al* 2003 *Plasma Phys. Control. Fusion* **45** A175
[19] Jarboe T R *et al* 2002 Progress with helicity injection current drive *19th IAEA Fusion Energy Conf. (Lyon)* IAEA-IC/P 10
[20] Tang X 2002 *8th International ST Workshop (18–21 November)* Princeton Plasma Physics Laboratory, Princeton, NJ
[21] Ono M and Choe W Out-board 'Ohmic induction' coil for low-aspect-ratio toroidal plasma start-up *Princeton University Patent Disclosure* 03-2003-1
[22] Lloyd B *et al* 1991 *Nucl. Fusion* **31** 2031
[23] Takase Y *et al* 2002 *J. Plasma Fusion Res.* **78** 719–21
[24] Ono M 1995 *Phys. Plasmas* **2** 4075
[25] Ryan P M *et al* 2002 IAEA-CN-94/EX/P2-13, Lyon, France
[26] Medley S *et al* 2003 *Proc. 30th Conf. on Plasma Physics and Controlled Fusion (St Petersburg, Russia, 7–11 July) (Europhysics Conference Abstracts)*
[27] Taylor G *et al* 2003 *Phys. Plasmas* **10** 1395
[28] Jones B *et al* 2003 *Phys. Rev. Lett.* **90** 165001